

1 **Organic Semiconducting Nanoprobe with Redox-Activatable NIR-II Fluorescence for In Vivo**  
2 **Real-time Monitoring drug-toxicity**

3

4 Yufu Tang <sup>a</sup>, Yuanyuan Li <sup>a</sup>, Zhen Wang <sup>a</sup>, Feng Pei <sup>b</sup>, Xiaoming Hu <sup>a</sup>, Yu Ji <sup>a</sup>, Xiang Li <sup>a</sup>, Hui Zhao  
5 <sup>a</sup>, Wenbo Hu <sup>a</sup>, Xiaomei Lu <sup>b</sup>, Quli Fan <sup>\*a</sup> and Wei Huang <sup>a,b,c</sup>

6

7 <sup>a</sup>Key Laboratory for Organic Electronics and Information Displays & Jiangsu Key Laboratory for  
8 Biosensors, Institute of Advanced Materials (IAM), Jiangsu National Synergetic Innovation Center  
9 for Advanced Materials (SICAM), Nanjing University of Posts & Telecommunications (NUPT),  
10 Nanjing 210023, China.

11 E-mail: iamqlfan@njupt.edu.cn

12 <sup>b</sup>Key Laboratory of Flexible Electronics (KLOFE), Institute of Advanced Materials (IAM), Jiangsu  
13 National Synergetic Innovation Center for Advanced Materials (SICAM), Nanjing Tech University  
14 (Nanjing Tech), Nanjing 211816, China

15 <sup>c</sup>Shaanxi Institute of Flexible Electronics (SIFE), Northwestern Polytechnical University (NPU),  
16 Xi'an 710072, China.

17

18

19 **1. Supplementary Figures**

20 **2. Materials**

21 **3. Characterization**

22 **4. Synthesis of probe (AOSNP)**

23 **5. NIR fluorescence spectroscopy.**

24 **6. The measured method of the fluorescence quantum yield**

25 **7. Cell culture.**

26 **8. Cell Viability Assay.**

27 **9. Procedure for cell imaging**

28 **10. In vivo blood elimination kinetics**

29 **11. In vivo NIR-II fluorescence monitoring APAP-induced**  
30 **hepatotoxicity**

31

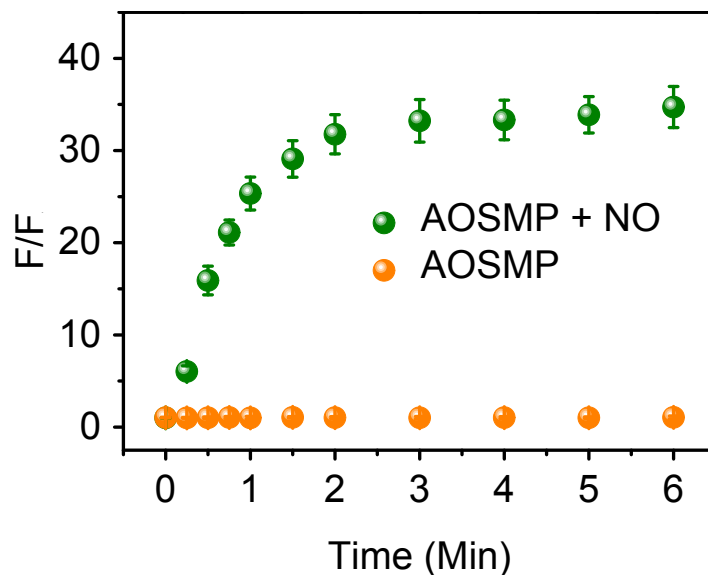
32

1

2

### 3 1. Supplementary Figures

4

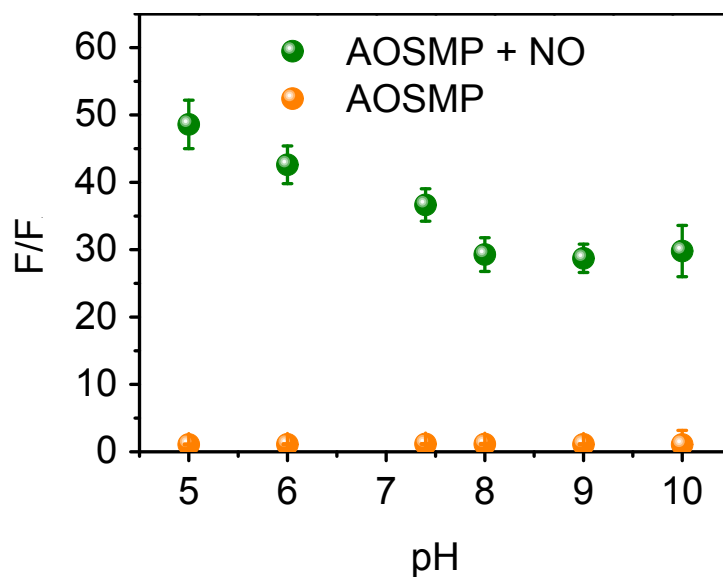


5

6

7 Supporting Figure S1. The ratiometric NIR-II fluorescence intensity ( $F/F_0$ ) of the  
8 AOSMP ( $3 \mu\text{g mL}^{-1}$ ) as a function of time in the presence of NO ( $100 \mu\text{M}$ ).

9



10

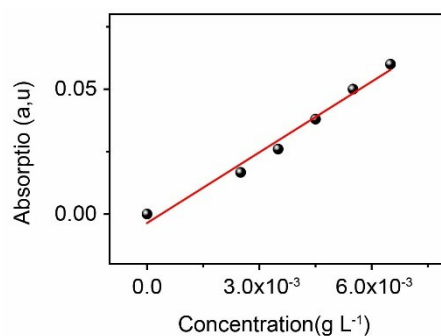
11 Supporting Figure S2. The influence of pH to the ratiometric NIR-II fluorescence  
12 intensity ( $F/F_0$ ) of the AOSMP ( $3 \mu\text{g mL}^{-1}$ ) in the absence (orange) or presence (olive)  
13 of NO ( $35 \mu\text{M}$ ).

14

15

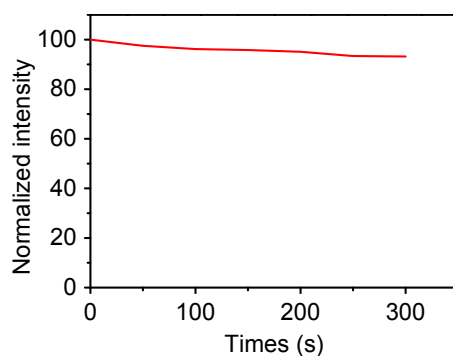
16

17



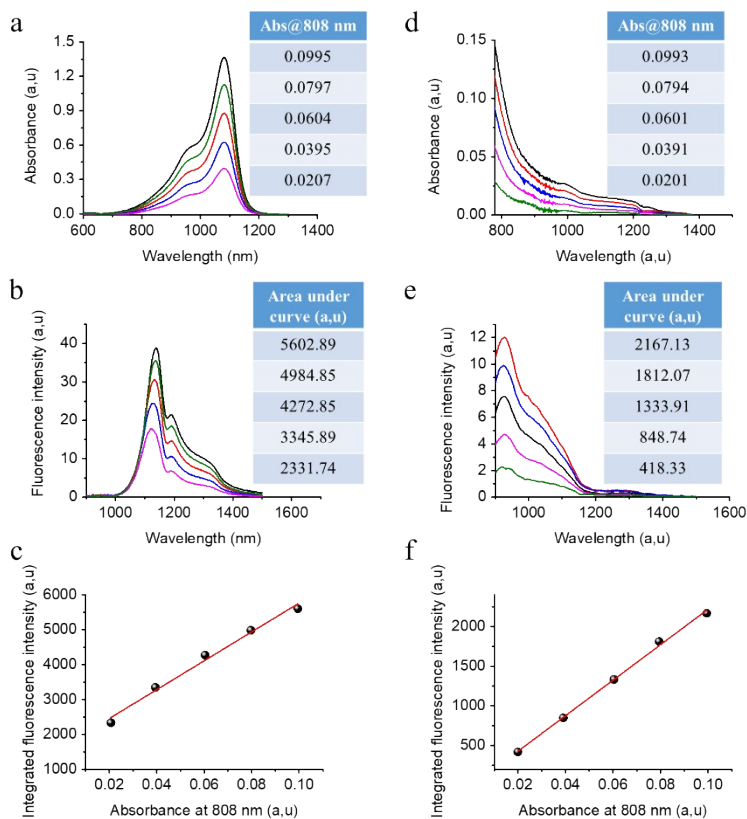
1

2 Supporting Figure S3. The mass extinction coefficient of AOSNP-NO (AOSNO after  
3 addition of excess NO).



4

5 Supporting Figure S4. The decay of fluorescence intensity of AOSNP-NO in PBS under  
6 continuous 808 nm light irradiation at a power density of 0.3 W cm<sup>-2</sup> for even over 300  
7 s.

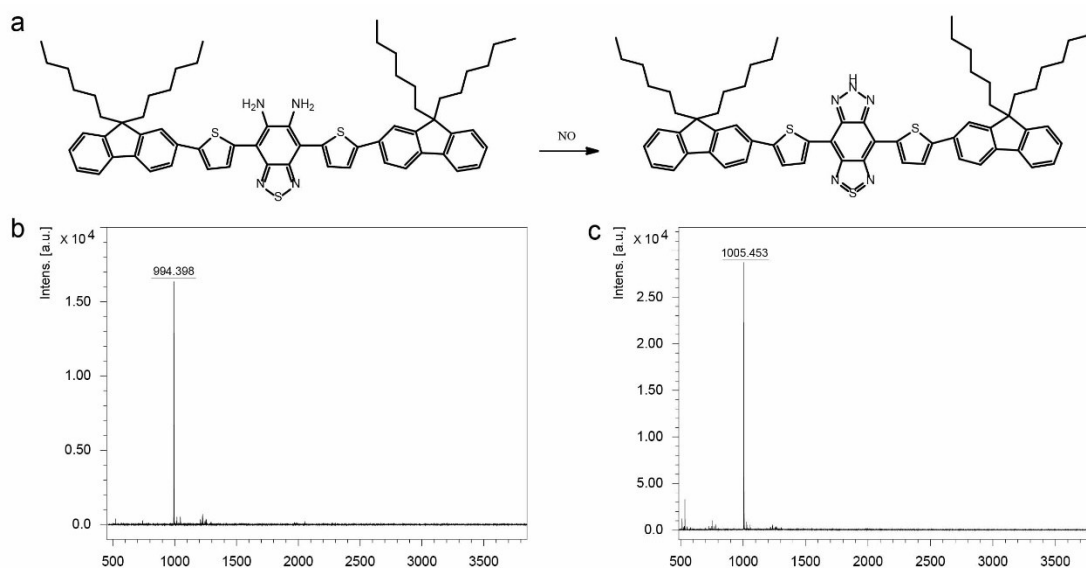


8

9 Supporting Figure S5. (a) The absorption spectra of different concentrations of IR-26

1 in 1,2-dichloroethane with absorbance values at 808 nm of  $\sim 0.10$  (Black),  $\sim 0.08$   
 2 (Green),  $\sim 0.06$  (Red),  $\sim 0.04$  (Blue) and  $\sim 0.02$  (Pink), respectively. A total of five  
 3 solutions with linearly spaced concentrations were loaded into a 10 mm fluorescence  
 4 cuvette one at a time, and the exact absorbance for each solution was listed in the inset  
 5 table. (b) The corresponding fluorescence spectra of above five solutions with  
 6 absorbance values at 808 nm. Their emission spectra were taken when the 808 nm laser  
 7 was used as the excitation and a 900 nm long-pass filter was used as the emission filter  
 8 to acquire the emission spectrum in the 900-1500 nm region, shown in black, green,  
 9 red, blue and pink, respectively. Area under curve in the emission spectra for each  
 10 solution was then calculated and listed in the inset table. (c) For all 1,2-dichloroethane  
 11 solutions of IR-26, their absorbance values were then plotted versus area under curve,  
 12 and fitted into a linear function, where slope of the fitted line was read as insert. (d-f)  
 13 The same absorption (d) and emission (e) measurements were performed for AOSNP-  
 14 NO nanoparticles in aqueous solutions. (f) Area under curve in the emission spectrum  
 15 of each solution of AOSNP-NO nanoparticles was then plotted against their absorbance  
 16 at 808 nm and fitted into a linear function, as slope was indicated.

17



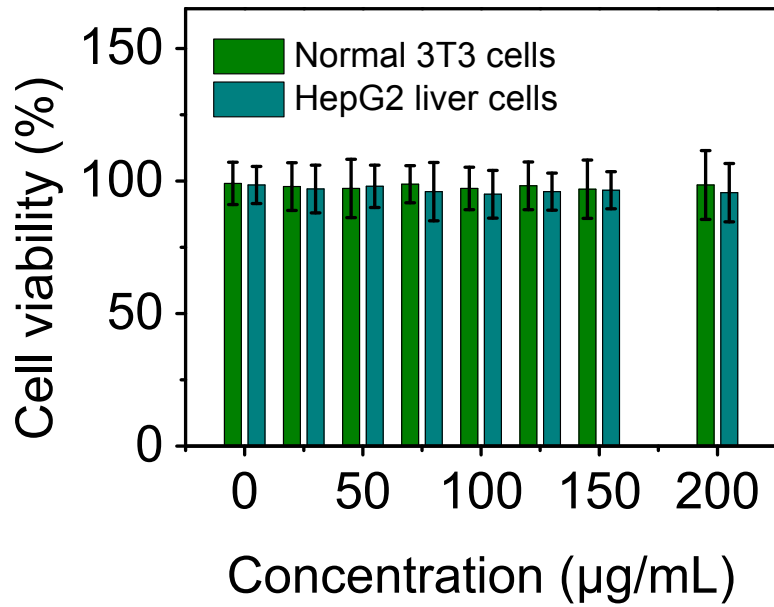
18

19 Supporting Figure S6. Possible mechanism of the model reaction between FTBD and  
 20 NO. (a) Proposed pathways for the reaction between FTBD and NO in aqueous  
 21 environment. The Matrix assisted laser desorption/ionization time-of-flight (MALDI-  
 22 TOF) mass spectrum of (b) FTBD and (c) NO-treated FTBD.

23

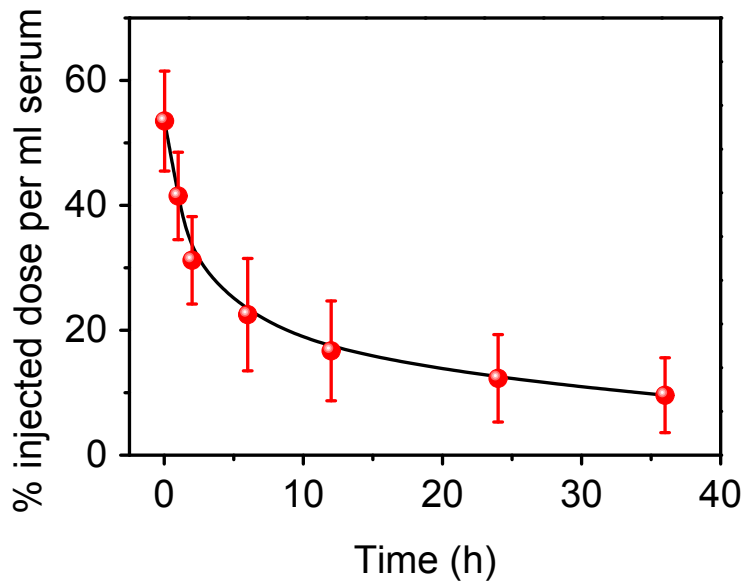
24

25



1

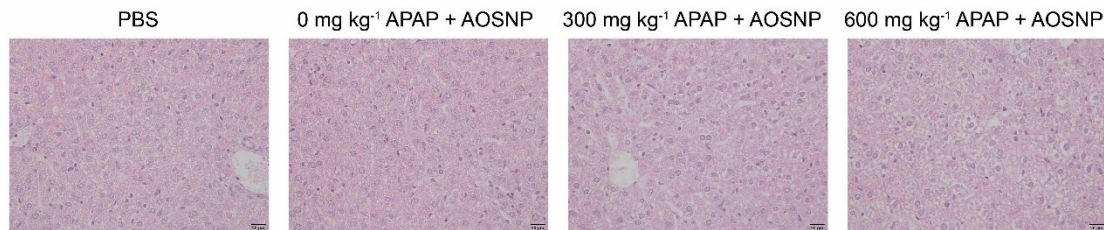
2 Supporting Figure S7. In vitro viability of normal 3T3 and HepG2 liver cells treated  
 3 with AOSMP solutions at different concentrations for 24 h.



4

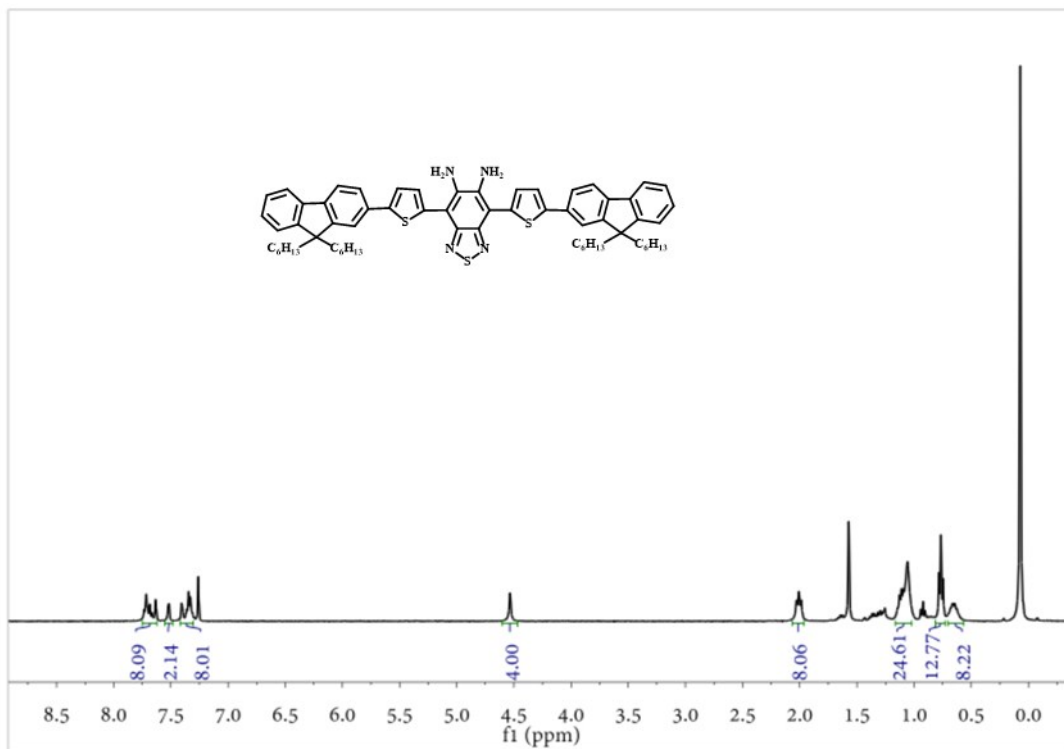
5 Supporting Figure S8. In vivo blood elimination kinetics of AOSMP at a dose of 100  
 6 µg per mouse (n = 3). The results were expressed as the mean ± s.d.

7



8

9 Supporting Figure S9. Representative hematoxylin and eosin staining (H&E) for liver  
 10 180 min after drug APAP administration (n = 3 mice per treatment group).



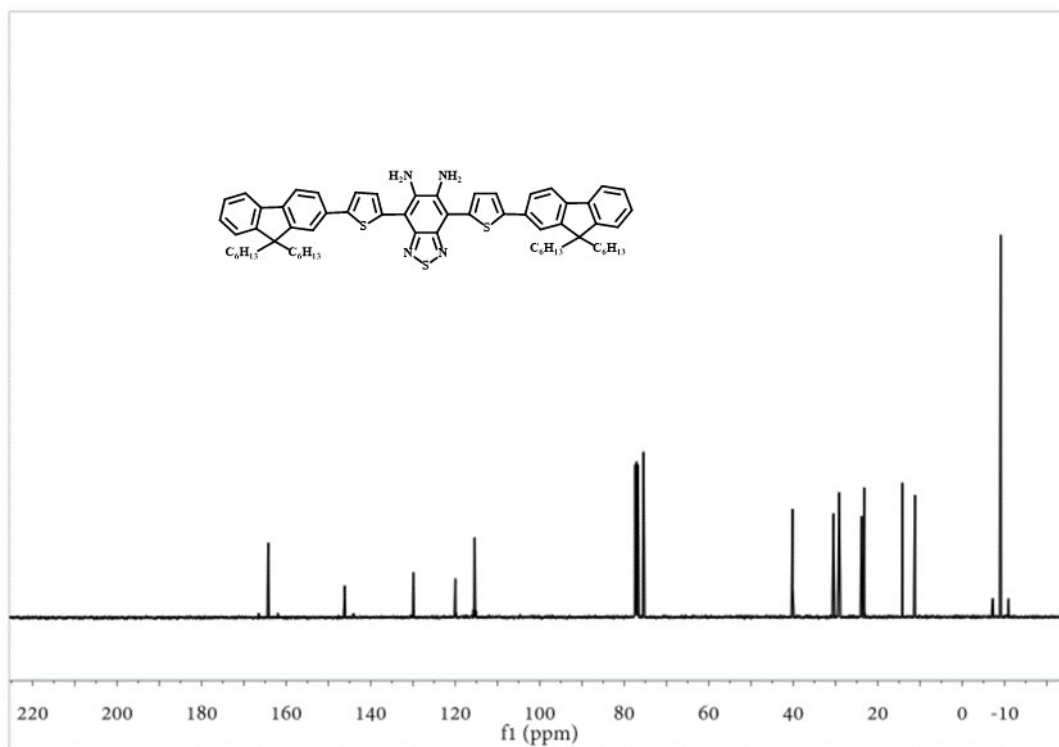
1

2 Supporting Figure S9. <sup>1</sup>H NMR Spectrum of the monomer FTBD in CDCl<sub>3</sub>.

3

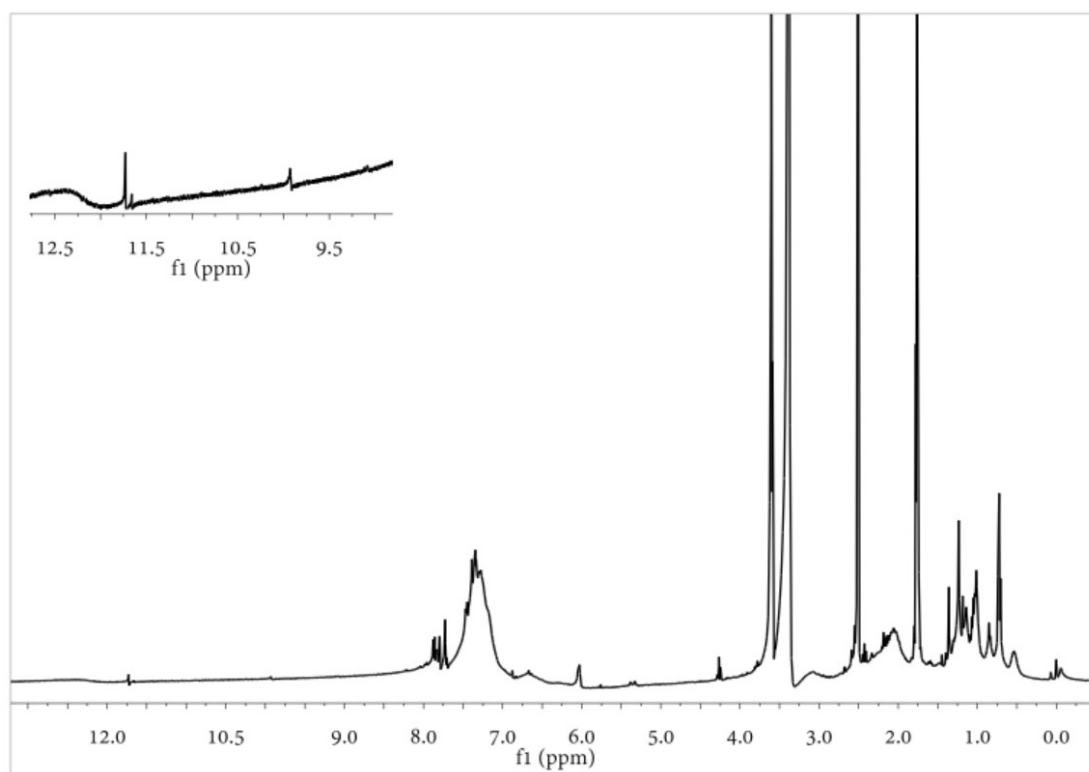
4

5



6

7 Supporting Figure S10. <sup>13</sup>C-NMR spectrum of the monomer FTBD in CDCl<sub>3</sub>.



1

2 **Supporting Figure S11.**  $^1\text{H}$ -NMR spectrum of the monomer PSMA-FTBD in DMSO-  
3 *d*<sub>6</sub>.

4 **2. Materials:** Unless otherwise noted, all reagents were purchased from Sigma Aldrich  
5 and used without additional purification. All reactions were carried out under nitrogen  
6 atmosphere. Tetrahydrofuran (THF) was purified and dried by passing through two  
7 columns of neutral alumina, under nitrogen, prior to use. All other solvents were  
8 purchased from either Fisher Scientific or Aldrich. The synthesis of monomers FTBD  
9 can be found in previous publications<sup>1</sup>.

10 **3. Characterization:** NMR spectra were recorded on a Bruker Ultra Shield Plus 400  
11 MHz spectrometer ( $^1\text{H}$ : 400 MHz,  $^{13}\text{C}$ : 100 MHz) and referenced to tetramethylsilane  
12 (TMS) as the internal standard. The absorption data and photoluminescence spectra  
13 were measured by a Shimadzu UV-3600 ultraviolet-visible-near-infrared  
14 spectrophotometer and an Edinburgh FLSP920 fluorescence spectrophotometer,

1 respectively. The laser source is a Ti:sapphire system that produced 100 fs pulses at a  
2 repetition of 80 MHz. All images were acquired on a home-built imaging set-up with  
3  $319 \times 256$  pixel two-dimensional InGaAs array (Princeton Instruments 2D OMA-V  
4 1.7; pixel number:  $319 \times 256$ ; readout noise: 50 electron r.m.s.; dark signal: 5,000  
5 electrons per second per pixel). Average molecular weights ( $M_w$ ,  $M_n$ ) were  
6 determined by Gel permeation chromatography (GPC) against polystyrene standards.  
7 THF was used as eluent with a flow rate of 1ml/min. Monomers were synthesized  
8 according to the reported methods. Dynamic light scattering (DLS) studies were  
9 conducted using ALV/CSG-3 laser light scattering spectrometers at a scattering angle  
10 of  $90^\circ$ . Transmission electron microscopy (TEM) imaging was performed by using a  
11 HT7700 transmission electron microscope operating at an acceleration voltage of 100  
12 kV.

#### 13 **4. *Synthesis of probe (AOSNP)***

14 The synthesis of monomers FTBD can be found in previous publications<sup>1</sup>. FTBD (3  
15 mg) and PSMA (9 mg) were dissolved in anhydrous tetrahydrofuran (THF, 50 mL).  
16 Then the mixture was kept stirring under reflux and N<sub>2</sub> flow protection. The resultant  
17 solution was evaporated to remove solvent. Furthermore, the product was dissolved in  
18 pure water and then filtered through 0.22  $\mu\text{m}$  membrane. The aqueous solution was  
19 freeze drying. Next, the FTBD-pendant PSMA polymer was dissolved in PBS, and the  
20 concentration of the obtained solution was adjusted to 1 mg/mL for subsequent  
21 application.

#### 22 **5. NIR fluorescence spectroscopy.**



1 NIR fluorescence spectra were taken on an Edinburgh FLSP920 fluorescence  
2 spectrophotometer in the 900-1350 nm region when excited by an 808-nm laser. The  
3 excitation light at 808 nm was provided by an 808-nm diode laser (Ti:sapphire system  
4 lasers) at a total output power of 180 mW and filtered through an 900-nm long-pass  
5 filter (Thorlabs). The excitation laser beam was allowed to pass through the solution  
6 sample in PBS solutions (pH = 7.4) in a 1 mm path cuvette and the emission was  
7 collected with the transmission geometry. A 900-nm long-pass filter alone was used to  
8 reject the excitation light at 808 nm. The emission spectrum was corrected after raw  
9 data acquisition to take into account the detector sensitivity profile and the extinction  
10 features of the filters.

## 11 **6. The measured method of the fluorescence quantum yield**

12 The fluorescence quantum yield of the AOSNP-NO was measured following a  
13 previously published protocol,<sup>2</sup> which utilizes the IR-26 whose quantum yield has been  
14 reported as 0.5 %. In a typical procedure, a stock solution of IR-26 in 1,2-  
15 dichloroethane was diluted in 1,2-dichloroethane until reaching an absorbance value of  
16 ~ 0.10 at 808 nm. A serial dilution of the sample was performed, yielding a total of five  
17 solutions with absorbance values at 808 nm of ~0.08, ~0.06, ~0.04 and ~0.02, which  
18 were subsequently confirmed with UV-Vis-NIR. NIR emission spectra of the five  
19 solutions with linearly spaced concentrations (including the first one with absorbance  
20 of ~0.10 at 808 nm) were taken in the same setup described in the preceding paragraph.  
21 The 808 nm laser was used as the excitation source and a 900-nm long-pass filter was  
22 used as the emission filter to acquire the emission spectrum in the 900-1500 nm region.  
23 Identical absorption and emission measurements were performed for AOSNP-NO in

1 aqueous solutions. All emission spectra were corrected after raw data acquisition to  
2 account for the detector sensitivity profile and the extinction features of the filters, and  
3 integrated in the 1000-1500 nm region. The integrated fluorescence intensity was  
4 plotted against absorbance at 808 nm (the excitation wavelength) and fitted into a linear  
5 function. Two slopes, one obtained for the IR-26 1,2-dichloroethane reference and the  
6 other from the AOSNP-NO nanoparticle sample, were used in the calculation of the  
7 quantum yield of AOSNP-NO nanoparticle in water, according to the following  
8 equation,

$$9 \quad QY_{\text{sample}} = QY_{\text{ref}} \cdot \frac{\text{slope}_{\text{sample}}}{\text{slope}_{\text{ref}}} \cdot \left( \frac{n_{\text{sample}}}{n_{\text{ref}}} \right)^2$$

10 where  $QY_{\text{ref}}$  is 0.5 % and  $n_{\text{sample}}$  and  $n_{\text{ref}}$  are the refractive index of water and 1,2-  
11 dichloroethane.

## 12 **7. Cell culture.**

13 3T3 and HepG2 liver cells were incubated respectively in DMEM supplemented with  
14 medium containing 10% fetal bovine serum (FBS) and 1% penicillin/streptomycin at  
15 37 °C in a humidified atmosphere of 5% CO<sub>2</sub> for 24 h.

## 16 **8. Cell Viability Assay.**

17 The MTT assay was used to determine the in vitro cytotoxicity of AOSNP in normal  
18 3T3 and HepG2 liver cells. The cells were inculcated in medium containing different  
19 doses of AOSNP for 24 h. After that, 10 μL MTT (0.5 mg/mL) solution was added into  
20 each well. After 3 h incubation at 37 °C, the supernatant was removed and 200 μL of  
21 dimethyl sulfoxide (DMSO) was added. A PowerWave XS/XS2 microplate  
22 spectrophotometer was used to record the absorbance intensity at 490 nm. The cellular

1 viability relative to the control group (PBS treated cells) was calculated as  $A_{\text{sample}}$   
2  $/A_{\text{control}}$ , in which  $A_{\text{sample}}$  and  $A_{\text{control}}$ , respectively, represent the average absorption of  
3 groups containing SPNP25 and control cells.

#### 4 **9. Procedure for cell imaging.**

5 Approximately  $5 \times 10^5$  HepG2 liver cells were seeded respectively in 6-well culture  
6 plates per well and cultured overnight. Then, the cells grew till 80 ~ 90% confluency  
7 and washed with PBS. AOSNP group: Cells were treated with AOSNP ( $5 \mu\text{g mL}^{-1}$ ) for  
8 30 min. Experimental group: Cells were treated with 250 and 500  $\mu\text{M}$  APAP for 1 h,  
9 respectively, and then added with AOSNP ( $5 \mu\text{g mL}^{-1}$ ) for 30 min. Remediation effect  
10 of NAC: Cells were firstly cultured with NAC (1.0 mM) for 1 h, and then treated with  
11 600  $\mu\text{M}$  APAP for 1h, followed by stained with AOSM ( $5.0 \mu\text{g mL}^{-1}$ ) for 30 min. Cell  
12 imaging was collected at 1000 ~ 1700 nm by using a Ti-Sapphire laser excitation  
13 wavelength at 808 nm.

#### 14 **10. In vivo blood elimination kinetics.**

15 The jugular vein of male Sprague–Dawley rats was cannulated and a catheter was  
16 implanted for intravenous injection and blood collection. AOSNP were injected  
17 through the catheter. Whole blood samples (100  $\mu\text{L}$ ) were collected via jugular vein  
18 catheter before dosing and at predetermined time points post injection and used to detect  
19 SPNP25 concentration by the measurement of absorbance at 525 nm by a Shimadzu  
20 UV-3600 ultraviolet-visible-near-infrared spectrophotometer. The values were plotted  
21 versus time after the subtraction of blood background.

#### 22 **11. In vivo NIR-II fluorescence monitoring APAP-induced hepatotoxicity**

1 Different concentrations of APAP (300 and 600 mg kg<sup>-1</sup>) were performed  
2 intraperitoneal injection at a series of living mice. After 60 minutes, AOSNP (10 mg  
3 mL<sup>-1</sup>, 100 μL) was injected into the mice by the tail vein. Then the mice were  
4 anesthetized for NIR-II fluorescence imaging at different time points. The control mice  
5 with PBS and APAP (0 mg kg<sup>-1</sup>) treatment were also anesthetized for NIR-II  
6 fluorescence imaging at different time points. All mice were sacrificed and imaged  
7 abdominal cavity regions after dissection from the ventral aspect at 150 min post-  
8 injection. In vivo imaging was collected at 1000 ~ 1700 nm by using a Ti-Sapphire  
9 laser excitation wavelength at 808 nm (the exposure time (200 ms), power density  
10 (~100 mW cm<sup>2</sup> on the animal surface), fluence rate (50 W cm<sup>-2</sup>)).

11

- 12 1. G. Qian, B. Dai, M. Luo, D. B. Yu, J. Zhan, Z. Q. Zhang, D. G. Ma and Z. Y. Wang,  
13 *Chem. Mater.*, 2008, **20**, 6208.
- 14 2. A. L. Antaris, H. Chen, K. Cheng, Y. Sun, G. Hong, C. Qu, S. Diao, Z. Deng, X. Hu,  
15 B. Zhang, X. Zhang, O. K. Yaghi, Z. R. Alamparambil, X. Hong, Z. Cheng and  
16 H. Dai, *Nature materials*, 2016, **15**, 235.

17